Bull. Mater. Sci., Vol. 40, No. 7, December 2017, pp. 1435–1439
https://doi.org/10.1007/s12034-017-1509-7

Temperature effects on the electrical characteristics of Al/PTh–SiO_2/p-Si structure

DURMUŞ ALİ ALDEMİR*, ALİ KÖKCE and AHMET FARUK ÖZDEMİR
Department of Physics, Faculty of Science and Arts, Süleyman Demirel University, Isparta 32260, Turkey
*Author for correspondence (dalialdemir@gmail.com)

MS received 14 November 2016; accepted 24 April 2017; published online 6 December 2017

Abstract. The temperature-dependent current–voltage (I–V) and capacitance–voltage (C–V) characteristics of the fabricated Al/p-Si Schottky diodes with the polythiopene–SiO_2 nanocomposite (PTh–SiO_2) interlayer were investigated. The ideality factor of Al/PTh–SiO_2/p-Si Schottky diodes has decreased with increasing temperature and the barrier height has increased with increasing temperature. The change in the barrier height and ideality factor values with temperature was attributed to inhomogeneties of the zero-bias barrier height. Richardson plot has exhibited curved behaviour due to temperature dependence of barrier height. The activation energy and effective Richardson constant were calculated as 0.16 eV and 1.79×10^{-8} A cm^{-2} K^{-2} from linear part of Richardson plots, respectively. The barrier height values determined from capacitance–voltage–temperature (C–V–T) measurements decrease with increasing temperature on the contrary of barrier height values obtained from I–V–T measurements.

Keywords. Schottky barriers; polymers and organics; composite materials; metal–insulator–semiconductor structures.

1. Introduction

The electrical and optical modification of a metal–semiconductor contact can be made using an organic interlayer. The efficiency and feasibility of such hybrid material systems in electronic applications was studied by many researchers [1–4]. To fabricate devices with desirable properties, various polymeric materials were grown on inorganic semiconductors as thin film forms by the different methods (spin coating, plasma, dropping, etc.) before metal deposition [5–8].

Owing to their variety, low cost, easy manufacturing, optical and electrical merits, the conducting polymers, such as poly(acetylene)s, poly(prole)s, poly(thiophene)s (PTh) were studied by many researchers for potential applications in molecular electronics, light emitting diodes (LEDs), supercapacitors and Schottky diodes [9–11]. Among them, the polythiophene has wide application field due to its chemical variability, good environmental and thermal stability [9,10,12]. Conducting polymer-layered nanocomposites are materials including nanosized particles into a matrix of standard polymer material. A particular property of the polymer such as conductivity or wettabilty can be controlled by addition of nanoparticles [6,13,14]. Polymer-based SiO_2 nanocomposites have received great interest due to their potential applications in microelectronic and optical devices [15].

Aldemir *et al* [16] investigated the effects of a thin polythiophene–silicon dioxide (PTh–SiO_2) nanocomposite interlayer on the electrical characteristics of Al/p-Si Schottky diodes at room temperature. The diodes showed good rectifying behaviour. Schottky type diodes are sensitive to ambient temperature. Therefore, it is necessary that the current–voltage (I–V) and capacitance–voltage (C–V) characteristics of Al/PTh–SiO_2/p-Si Schottky diodes should be analysed in wide temperature before the diodes are used in the electrical and optical applications. Furthermore, the dominant conduction mechanism of the diodes can be determined using temperature-dependent measurements [17–19]. Hence, in the present work, I–V and C–V characteristics of the prepared Al/p-Si Schottky diodes with polythiophene–SiO_2 nanocomposite interlayer were analysed in wide temperature range.

2. Experimental

In this study, boron-doped p-type silicon wafer (100) with 5.64×10^{15} cm^{-3} carrier concentration was used. A wet chemical process was carried out to remove undesirable contaminations from Si surface. For this purpose, the wafer was cleaned with trichloroethylene, acetone and methanol. Then, the surface of Si were etched in $H_2SO_4 + H_2O_2 + H_2O$ (5:1:1), 20% HF, $HNO_3 + HF + H_2O$ (6:1:35) and 20% HF, consecutively [20]. After each step, the wafer was rinsed by deionized water with high resistivity. Al was evaporated to the back surface of Si for ohmic contact, followed by annealing.

A solution of PTh–SiO_2 polymer nanocomposite was prepared by dissolving 30 µg of PTh–SiO_2 in 1 µl

N-methyl-2-pyrrolidone. Before Schottky metallization of Al, the solution was spin-coated onto the front surface of the wafer at 500 rpm and dried under a nitrogen flow to remove the solvent. Thus, a thin layer of the PTh–SiO_2 polymer nanocomposite was deposited on the wafer. Schottky contacts were realized by the evaporation of Al at 2.7×10^{-5} Pa and the circular surface area of the Schottky contacts was 2×10^{-2} cm^2. The thickness of the thin film was calculated between 10.4 and 25.9 nm with the help of C–V measurements at 1 MHz (not shown here). The synthesis and characterization of PTh–SiO_2 polymer nanocomposite were discussed elsewhere [13]. I–V and C–V data were measured by the use of a Keithley Model 2400 SourceMeter and a HP4192A LF Impedance analyzer, respectively, at a wide temperature range, in dark. The low temperature I–V and C–V measurements were taken in a Leybold Heraeus closed-cycle helium cryostat. Controlling of the sample temperature was provided by a Windaus MD850 electronic thermometer and a copper constantan thermocouple.

3. Results and discussion

The semi-logarithmic plots of the forward bias I–V characteristics of Al/PTh–SiO_2/p-Si/Al Schottky diodes at various temperatures are shown in figure 1. As can be seen from the figure, the I–V curves are linear at low bias and the diodes show good rectifying behaviour for each temperature. Nevertheless, the observed variation in I–V curves as a function of temperature implies that the thermionic emission is the dominant current transport mechanism [21].

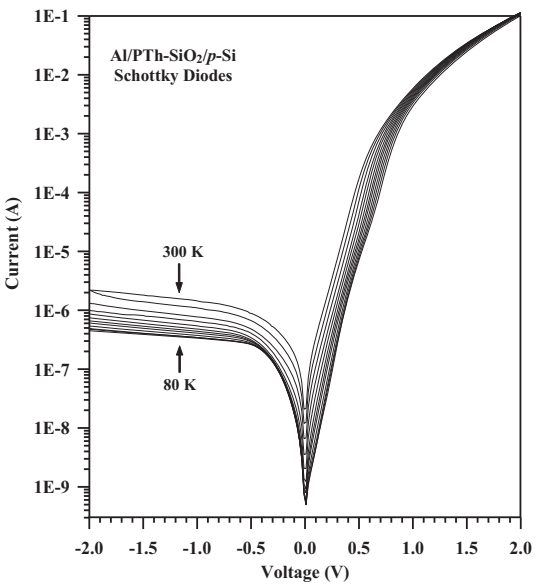

Figure 1. Forward and reverse bias C–V characteristics of Al/PTh–SiO_2/p-Si/Al Schottky diodes at different temperatures in the range 80–300 K.

For Schottky contacts, the relationship between voltage and current is expressed as [22]:

$$I = I_0 \left[\exp\left(\frac{qV}{nkT}\right) - 1 \right]. \tag{1}$$

Here q, n, k, T are the elementary charge, the ideality factor, the Boltzmann constant, the absolute temperature, respectively. The saturation current (I_0) is given as:

$$I_0 = AA^*T^2 \exp\left(-\frac{q\Phi_{bo}}{kT}\right). \tag{2}$$

In this equation, A and A^* are the contact area and the effective Richardson constant ($32\ A\,cm^{-2}\,K^{-2}$ for p-Si [3]), respectively. Φ_{bo} is the barrier height (BH) at zero-bias. The slope of the linear portion of semilog I–V characteristic gives value of n.

$$n = \frac{q}{kT}\frac{dV}{d\ln I}. \tag{3}$$

Φ_{bo} and n values were determined by using equations (2 and 3) for each temperature. Φ_{bo} and n values *vs*. temperature plots are given in figure 2. n value of 2.51 at 300 K offers that the existence of native oxide and the polymer interlayer between Al and p-Si causes the conversion of the device to the metal/insulator/semiconductor (MIS) device. Nano-sized SiO_2 particles content in PTh matrix affects morphological and electrical properties of the film [6,13]. As shown in ref. [13], the conductivity of chemically synthesized PTh–SiO_2 nanocomposite is smaller than PTh. This case can be attributed to the SiO_2 particles intercalated by the conducting PTh inducing a weak interchain interaction between the PTh chains [13,23]. As the temperature increases, the value of n decreases and the value of zero-bias BH increases. Similar results for Al/p-Si MIS diodes were reported in literature [24–26].

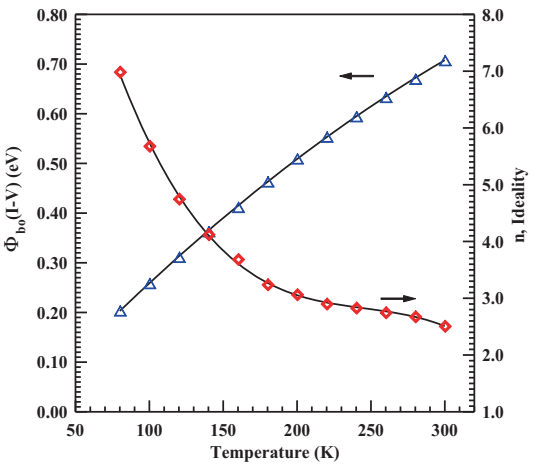

Figure 2. Variation of zero bias barrier height and ideality factor with temperature for Al/PTh–SiO_2/p-Si/Al Schottky diodes.

Table 1. Temperature coefficients for $E_g(T)$ and $\Phi_{bo}(T)$.

Paramaters	α (eV K^{-2})	β (eV K^{-2})	$E_g(0)$ or $\Phi_{bo}(0)$ (eV)
$E_g(T)$[1] $0 < T \leq 190$ K	-6.05×10^{-7}	1.06×10^{-5}	1.170
$E_g(T)$[1] $150 \leq T \leq 300$ K	-3.05×10^{-7}	-9.02×10^{-5}	1.179
$\Phi_{bo}(T)$	-2.53×10^{-6}	3.26×10^{-3}	−0.041

[1]Ref. [27].

Temperature dependence of silicon's band gap can be given in quadratic form as follows [27]:

$$E_g(T) = \alpha T^2 + \beta T + E_g(0). \quad (4)$$

Here α and β are temperature coefficients. $E_g(0)$ is the value of the band gap at absolute zero. If we assume that the temperature dependence of zero-bias BH has same form with E_g, equation (4) can be written as follows:

$$\Phi_{bo}(T) = \alpha T^2 + \beta T + \Phi_{bo}(0). \quad (5)$$

Here Φ_{bo} is the value of zero bias BH at absolute zero. The fitting results of equations (4 and 5) to the zero-bias BH and band gap *vs*. temperature data are given in table 1.

As we refer to values of α and β in table 1, the temperature dependence of zero-bias BH of the diodes is not corresponding to the change in the band-gap of Si with the temperature. According to Tung's model [28], some small patches with low Schottky BH are embedded in the area, where the Schottky BH is properly distributed. At low temperature, the charge carriers will tend to flow from the region including these patches. This causes lower apparent Schottky BHs and larger ideality factors. The current flow begins to occur from the regions including high Schottky barriers as well as low Schottky barriers as the temperature increases. As a result, there will be increase in zero-bias BH and decrease in ideality factor with increasing temperature [26,28,29]. Therefore, the temperature-dependent BH and ideality factor of the diodes can be attributed to inhomogeneties of the zero-bias BH [26,30]. The lateral variation of the organic layer thickness and non-uniformity of the interface charges can be responsible for the zero-bias BH inhomogeneties [31,32].

The usual Richardson plot of the diodes is shown in figure 3 and there is a deviation from linearity below 240 K due to strong temperature dependence of Φ_{bo} and n [33,34]. A^* and activation energy can be calculated from linear portion of $\ln(I_0/T^2)$ *vs.* $1/T$ plot. The values of activation energy and A^* were calculated as 0.14 eV and 1.10×10^{-8} A cm^{-2} K^{-2}, respectively. This value of A^* is too small when compared to 32 A cm^{-2} K^{-2} for p-Si. The lowering in value of A^* can be explained by the presence of the native oxide and the polymer interlayer between Al and p-Si [35]. This case is frequently encountered in the literature for metal/p-Si Schottky contacts with insulating interlayer [25,26].

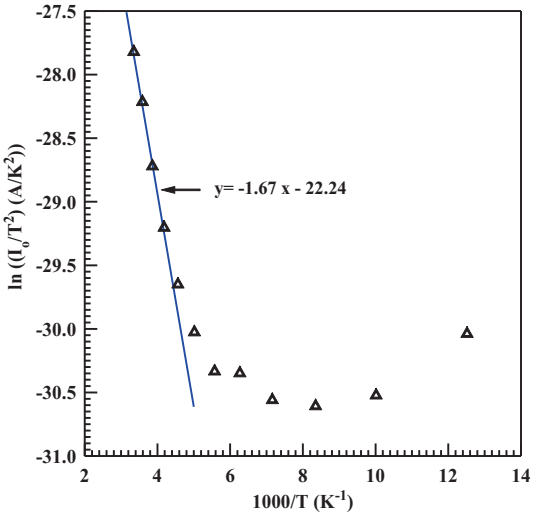

Figure 3. Richardson plot for Al/PTh−SiO_2/p-Si/Al Schottky diodes.

The reverse bias capacitance of a Schottky diode is given as [22,36]:

$$C^{-2} = \frac{2(V_d + V_r - kT/q)}{\varepsilon_s \varepsilon_0 q A^2 N_A}, \quad (6)$$

where V_d and V_r are the diffusion potential and the magnitude of the reverse bias, respectively. ε_0 (8.85×10^{-14} F cm^{-1}) is the permittivity of free space and ε_s (11.9 for Si [36]) is the relative permittivity of the semiconductor. The C^{-2}–V_r plot is linear for uniformly doped semiconductor and the acceptor concentration, N_A is determined from the slope of this plot by the following equation.

$$N_A = \frac{2}{\varepsilon_s q A^2 (d(C^{-2})/dV_r)}. \quad (7)$$

BH value from the C–V measurements is calculated by the relation,

$$\Phi_b(C\text{–}V) = V_d + \frac{kT}{q} \ln\left(\frac{N_v}{N_A}\right), \quad (8)$$

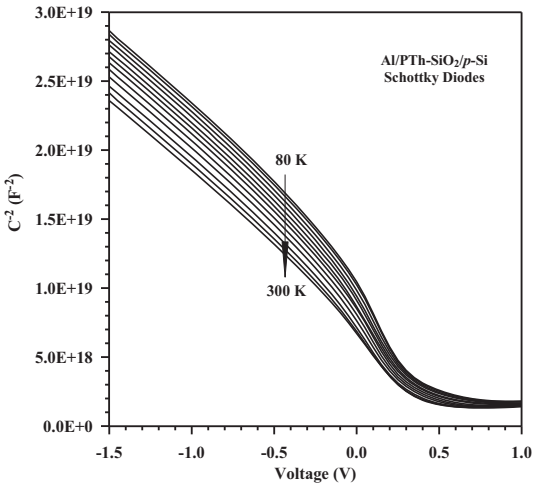

Figure 4. The reverse bias C^{-2}–V characteristics of Al/PTh−SiO_2/p-Si/Al Schottky diodes as a function of temperature.

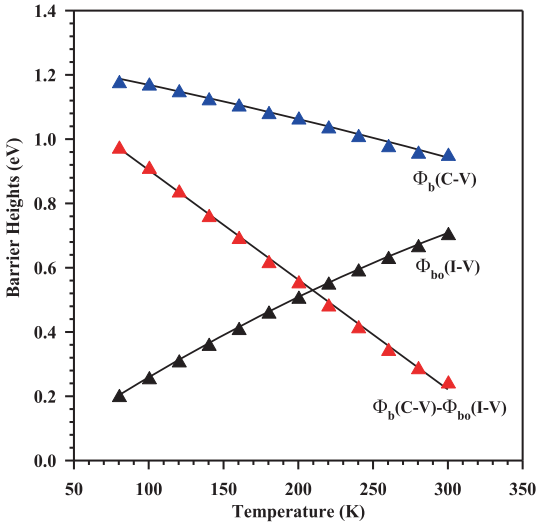

Figure 5. The temperature dependence of barrier heights obtained from I–V and C–V measurements of Al/PTh−SiO_2/p-Si/Al Schottky diodes.

here $N_v = 3.08 \times 10^{14}\, T^{3/2}\,\mathrm{cm}^{-3}$ is the effective density of states in Si valance band [37].

The temperature-dependent C–V measurements of the diodes were taken at 1 MHz to eliminate the additional capacitance caused by interface states [38]. The reverse bias $C^{-2}-V_r$ characteristics of the diodes over the temperature range of 80–300 K are shown in figure 4. The reverse bias capacitance of the diodes increases with increasing temperature. At low temperature, all most all the impurities are frozen out. Since the acceptor concentration increases with increasing temperature, the capacitance of the diodes increases with increasing temperature [39].

Figure 5 shows the temperature dependence of the barrier heights ($\Phi_b(C$–$V)$) calculated from linear region of reverse bias $C^{-2}-V_r$ characteristics by using equation (8). As can be seen in the figure, $\Phi_b(C$–$V)$ decreases with increasing temperature. The fitting of $\Phi_b(C$–$V) = \alpha T^2 + \beta T + \Phi_b(0)$ for BH *vs.* temperature data gives $\alpha = -6.79 \times 10^{-7}\,\mathrm{eV\,K^{-2}}$, $\beta = -8.60 \times 10^{-4}\,\mathrm{eV\,K^{-1}}$ and $\Phi_b(0) = 1.26\,\mathrm{eV}$. α and β coefficients are close agreement with coefficients reported for E_g in literature [27]. This result implies that the temperature dependence of $\Phi_b(C$–$V)$ is stem from the variation of E_g with temperature. For the sake of comparison, figure 5 also shows the variation of $\Phi_{bo}(I$–$V)$ and $\Phi_b(C$–$V) - \Phi_{bo}(I$–$V)$ with the temperature. For each temperature value, BH value calculated from C^{-2}–V_r characteristic is larger than BH value determined from I–V characteristic. This discrepancy can be attributed to Schottky BH inhomogeneties, PTh–SiO_2 interlayer and different natures of I–V and C–V measurements [29,40,41]. The junction current at the inhomogeneous metal–semiconductor interfaces is dominated by the low Schottky BH patches. Thus, the apparent Schottky BHs determined from dc I–V data are lower than the arithmetic weighed average of the entire diode [28]. Sullivan *et al* [42] show that the BH value obtained from C–V measurement is affected by the distribution of charge at the depletion region boundary. The distribution of this charge tracks the weighed arithmetic average of the Schottky BH inhomogeneity. Therefore, the Schottky BH obtained from C^{-2}–V plot agrees with the weighed arithmetic average of the Schottky BH [28,42,43]. As it is seen clearly, the Schottky BH values determined by I–V measurements will be usually lower than those obtained from the C–V measurements.

Some theoretical studies were conducted to reveal the cause of inconsistency between $\Phi_b(C$–$V)$ and $\Phi_{bo}(I$–$V)$ [28,42, 43]. Werner and Güttler [43] have developed a model, which assumes that the Schottky BH between metal and semiconductor has a Gaussian distribution. In this model, $\Phi_b(C$–$V) - \Phi_{bo}(I$–$V)$ difference is proportional to T^{-1}. Some experimental results have supported this case [37,44,45]. However, as can be seen in figure 5, $\Phi_b(C$–$V) - \Phi_{bo}(I$–$V)$ difference shows linear dependence on the temperature as different from the literature. This behaviour can be attributed to PTh−SiO_2 interlayer used between Al and p-Si.

4. Conclusions

The values of Φ_{bo} and n determined from I–V curves of Al/PTh–SiO_2/p-Si/Al Schottky diodes have exhibited temperature-dependent behaviour. This behaviour has been attributed to zero-bias BH inhomogeneties. The thickness difference of the PTh–SiO_2 organic interlayer from region to region can be caused the zero-bias BH inhomogeneties. The inhomogeneties in zero-bias barrier height can be reduced by using different methods instead of dropping-spin coating method which were used to grow organic layer on semiconductor surface. The effective Richardson constant is found to

be too small when compared to 32 A cm^{-2} K^{-2} for *p*-Si due to the existence of PTh–SiO_2 nanocomposite organic interlayer. The variation in $\Phi_b(C–V)$ values with the temperature is controlled by the temperature dependence of Si band-gap. The existence of PTh–SiO_2 nanocomposite interlayer affects the temperature dependence of $\Phi_b(C–V) - \Phi_{bo}(-V)$ difference.

Acknowledgements

We thank Ayşegül Öksüz, E Derya Koçak and Sibel Aydoğdu, who synthesized the polythiophene–SiO_2 nanocomposite.

References

[1] Farag A A M, Gunduz B, Yakuphanoglu F and Farooq W A 2010 *Synth. Met.* **160** 2559
[2] Ginev G, Riedl T, Parashkov R, Johannes H-H and Kowalsky W 2004 *Appl. Surf. Sci.* **234** 22
[3] Gupta R K, Aydın M E and Yakuphanoglu F 2011 *Synth. Met.* **161** 2355
[4] Kampen T U, Park S and Zahn D R T 2002 *Appl. Surf. Sci.* **190** 461
[5] Soylu M and Yakuphanoglu F 2012 *Superlattices Microstruct.* **52** 470
[6] Nastase F, Stamatin I, Nastase C, Mihaiescu D and Moldovan A 2006 *Prog. Solid State Chem.* **34** 191
[7] Chen C H and Shih I 2006 *J. Mater. Sci. Mater. Electron.* **17** 1047
[8] Özdemir A F, Aldemir D A, Kökce A and Altindal S 2009 *Synth. Met.* **159** 1427
[9] Ates M, Karazehir T and Sarac A S 2012 *Curr. Phys. Chem.* **2** 224
[10] Berggren M, Inganäs O, Gustafsson G, Rasmusson J, Andersson M R, Hjertberg T *et al* 1994 *Nature* **372** 444
[11] Saxena V and Santhanam K S 2003 *Curr. Appl. Phys.* **3** 227
[12] Kutsche C, Targove J and Haalandc P 1993 *J. Appl. Phys.* **73** 2602
[13] Gök A, Koçak E D and Aydoğdu S 2005 *J. Appl. Polym. Sci.* **96** 746
[14] Huang Z M, Zhang Y Z and Kotaki M 2003 *Compos. Sci. Technol.* **63** 2223
[15] Jeon I Y and Baek J B 2010 *Materials* (*Basel*) **3** 3654
[16] Aldemir D A, Esen M, Kökce A, Karataş S and Özdemir A F 2011 *Thin Solid Films* **519** 6004
[17] Cova P, Singh A and Masut R A 1997 *J. Appl. Phys.* **82** 5217
[18] Hübers H and Röser H 1998 *J. Appl. Phys.* **84** 5326
[19] Huang S and Lu F 2006 *Appl. Surf. Sci.* **252** 4027
[20] Aydin S B, Yildiz D E, Çavuş H K and Şahingöz R 2014 *Bull. Mater. Sci.* **37** 1563
[21] Hudait M K, Venkateswarlu P and Krupanidhi S B 2001 *Solid State Electron.* **45** 133
[22] Rhoderick E H and Williams R H 1988 *Metal–semiconductor contacts* (Oxford (England): Oxford University Press)
[23] Kim B H, Jung J H, Hong S H, Kim J W, Choi H J and Joo J 2001 *Synth. Met.* **121** 1311
[24] Altındal Ş, Dökme İ, Bülbül M M, Yalçın N and Serin T 2006 *Microelectron. Eng.* **83** 499
[25] Yüksel Ö F 2009 *Phys. B Condens. Matter* **404** 1993
[26] Huang W C, Horng C T, Cheng J C and Chen C C 2011 *Microelectron. Eng.* **88** 597
[27] Bludau W, Onton A and Heinke W 1974 *J. Appl. Phys.* **45** 1846
[28] Tung R T 1992 *Phys. Rev. B* **45** 13509
[29] Karataş Ş, Altındal Ş, Türüt A and Çakar M 2007 *Phys. B Condens. Matter* **392** 43
[30] Yakuphanoglu F 2007 *Phys. B Condens. Matter* **389** 306
[31] Tugluoglu N, Karadeniz S, Sahin M and Safak H 2004 *Appl. Surf. Sci.* **233** 320
[32] Aydoğan Ş, Sağlam M and Türüt A 2008 *Microelectron. Eng.* **85** 278
[33] Bhuiyan A S, Martinez A and Esteve D 1998 *Thin Solid Films* **161** 93
[34] Missous M and Rhoderick E H 1991 *J. Appl. Phys.* **69** 7142
[35] Srivastava A K, Arora B M and Guha S 1981 *Solid State Electron.* **24** 185
[36] Sze S M and Ng K K 2007 *Physics of semiconductor devices*, 3rd edn. (USA: Wiley-Interscience)
[37] Zeyrek S, Altındal Ş, Yüzer H and Bülbül M M 2006 *Appl. Surf. Sci*. **252** 2999
[38] Hudait M K and Krupanidhi S B 2001 *Mater. Sci. Eng. B Solid-State Mater. Adv. Technol*. **87** 141
[39] Khurelbaatar Z, Shim K, Cho J, Hong H, Reddy V R and Choi C 2015 *Mater. Trans*. **56** 10
[40] Pattabi M, Krishnan S, Ganesh and Mathew X 2007 *Sol. Energy* **81** 111
[41] Selçuk A, Ocak S B and Karadeniz S 2012 *Am. J. Mater. Sci.* **2** 125
[42] Sullivan J P, Tung R T, Pinto M R and Graham W R 1991 *J. Appl. Phys*. **70** 7403
[43] Werner J H and Güttler H H 1991 *J. Appl. Phys*. **69** 1522
[44] Karataş Ş, Altındal Ş and Çakar M 2005 *Phys. B Condens. Matter* **357** 386
[45] Janardhanam V, Kumar A A, Reddy V R and Reddy P N 2009 *J. Alloys Compd*. **485** 467